

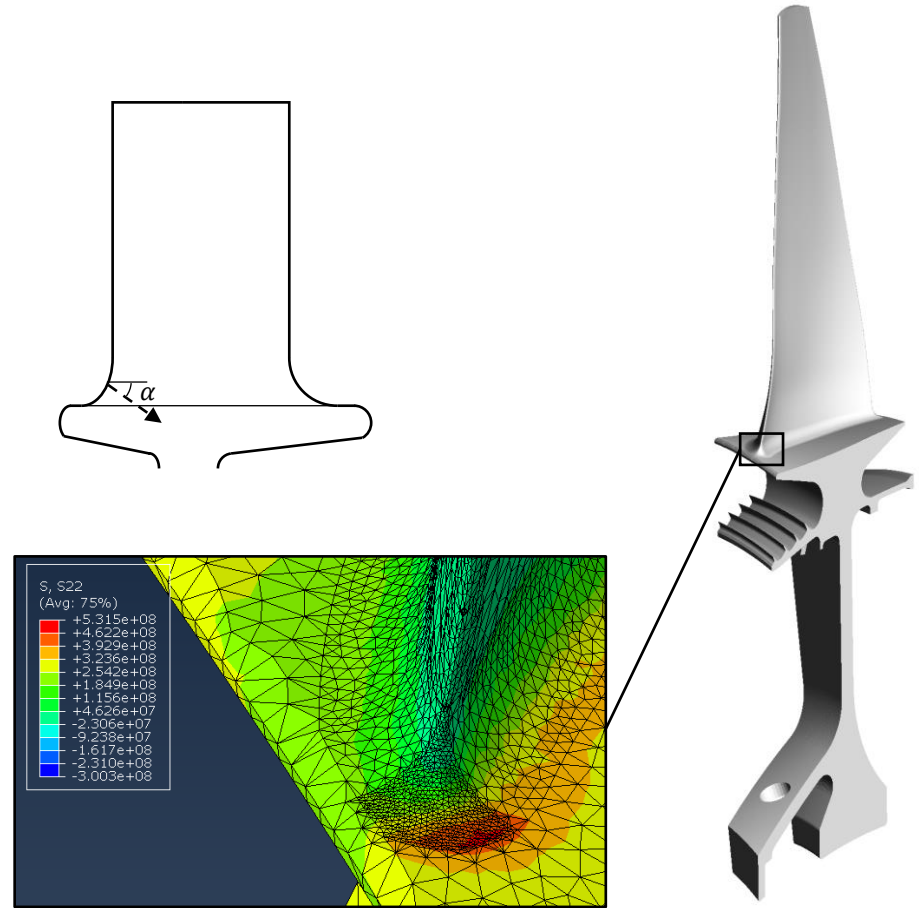
Multiaxial Crack Growth Prediction

Author: Bemin Sheen

Supervisor: Professor David Nowell

Problem overview

- Foreign object damage (FOD) in the fillet region of the leads to crack growth
- Depending on the location of the crack it may propagate to the bore of the disk



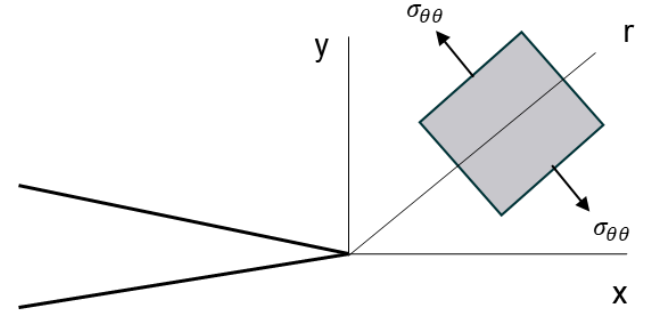
Objectives

- Design an experimental geometry to replicate the features of non-proportional crack propagation in aeroengine disks
- Carry out experiments to establish practical growth trajectories under controlled conditions
- Develop an improved criterion for the prediction of crack direction and, if possible, growth rate

Crack growth mechanism

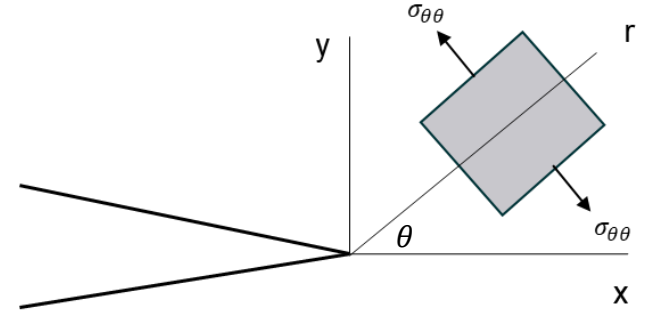
- Different crack direction criteria available
- Correct criterion is material dependent
- Transition between criteria is possible
- Maximum tensile stress:

$$- \sigma_{\theta\theta} = \frac{1}{\sqrt{2\pi r}} \cos\left(\frac{\theta}{2}\right) \left[\Delta K_I \cos\left(\frac{\theta}{2}\right) - \frac{3}{2} \Delta K_{II} \sin(\theta) \right]$$



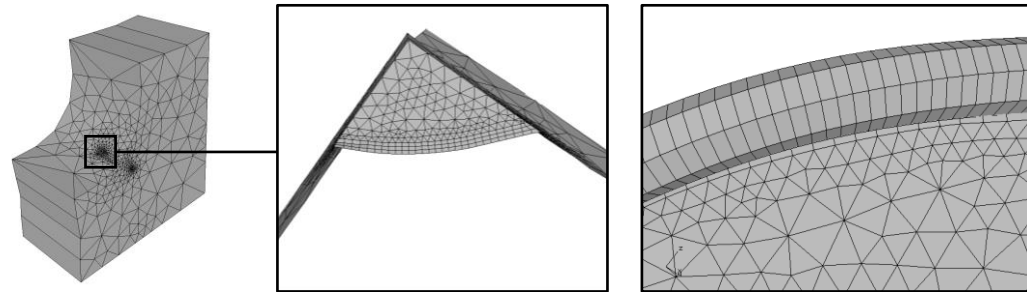
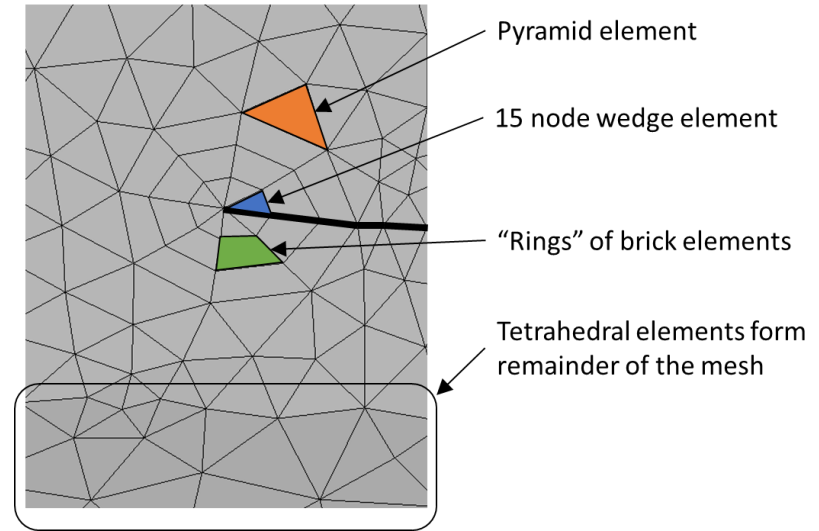
Non-proportional loading

- Non-proportional loading affects growth rate and trajectory
- Variable mode-mixity
 - Multiple local load maxima in one cycle
- Crack tip shielding



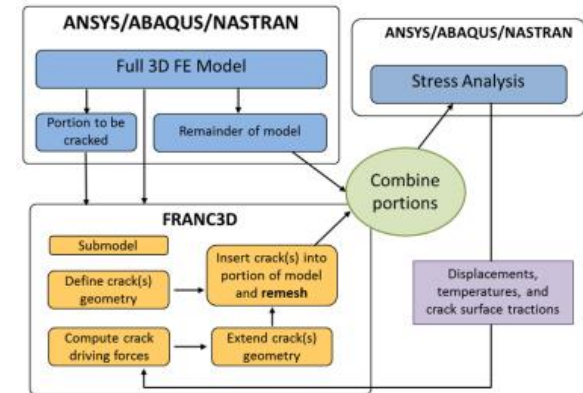
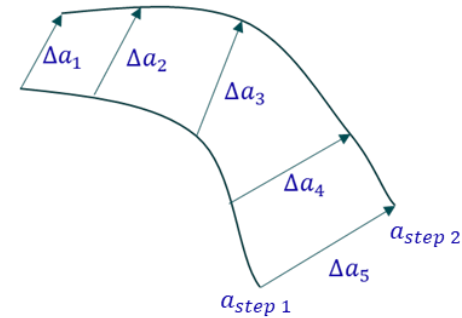
Crack modelling approach

- Contour integral to compute stress intensity factors (SIFs) in Abaqus + FRANC3D
- Incremental crack growth through remeshing
- Limited non-proportional crack growth modelling



Crack modelling approach

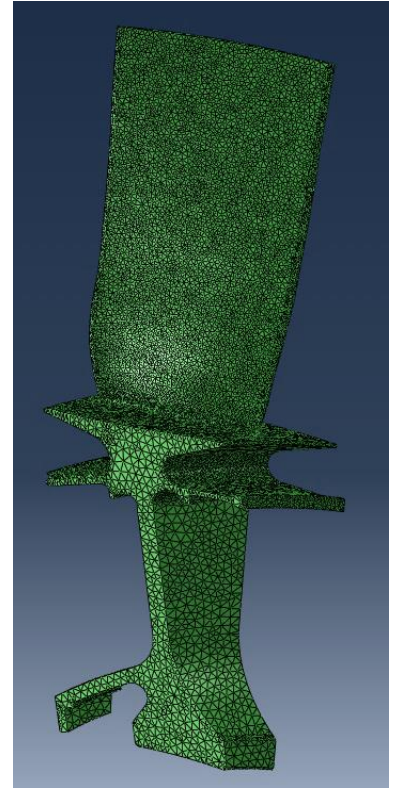
- Contour integral to compute stress intensity factors (SIFs) in Abaqus + FRANC3D
- Incremental crack growth through remeshing
- Limited non-proportional crack growth modelling



FRANC3D workflow [1]

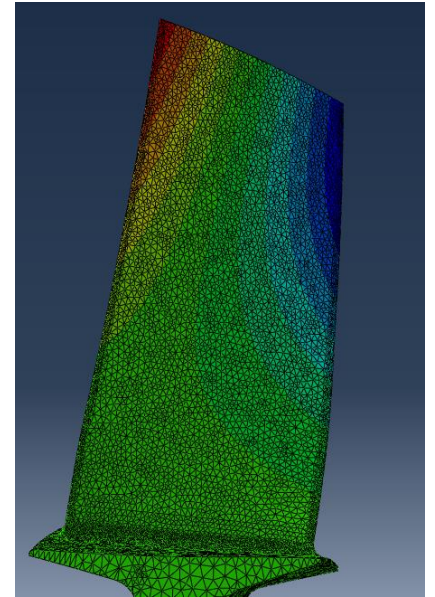
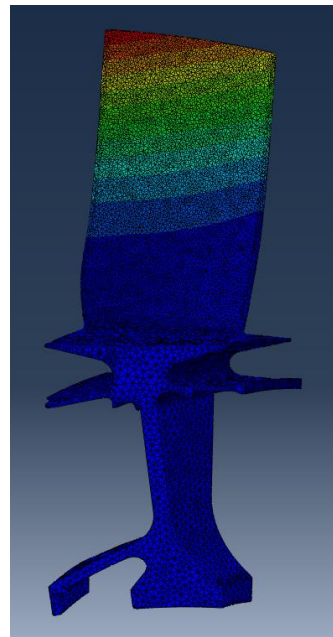
Loading

- Crack is subject to mixed-mode I/II/III loading
- LCF loading: rotational and thermal loads
- HCF loading: vibration



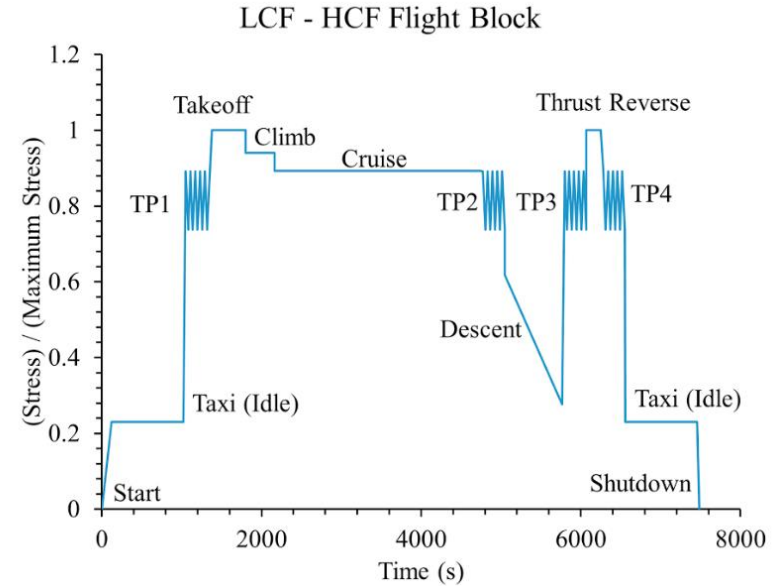
Mode shapes

- Static mode shapes:
 - 1st flap: 198.15 Hz
 - 1st torsion: 672.46 Hz



Crack growth mechanism

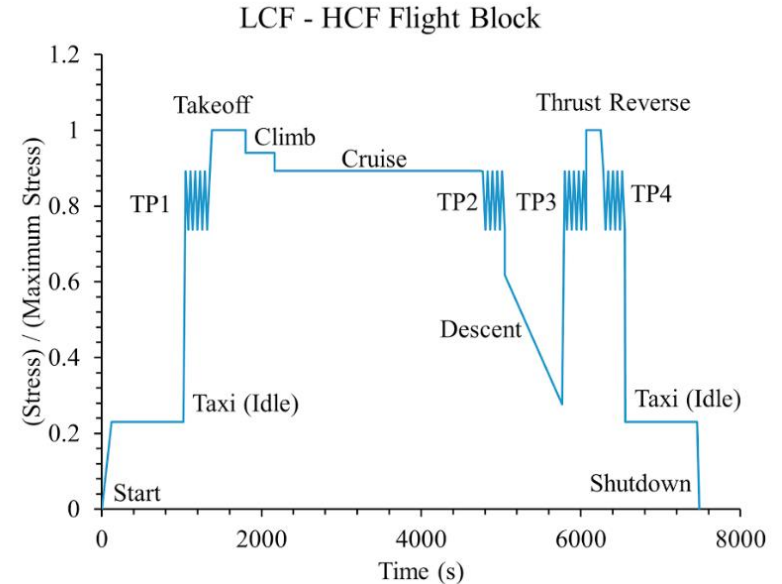
- Combination of high-cycle and low-cycle loading
- Previous work on compressor blades showed HCF to be the primary mechanism of fracture [2]
- Initial LCF growth until HCF threshold
- Subsequent HCF + LCF



Minor cycle of 'Descent-Thrust Reverse-Taxi' and a major cycle of 'Start-Takeoff-Shutdown' [1]

Crack growth mechanism

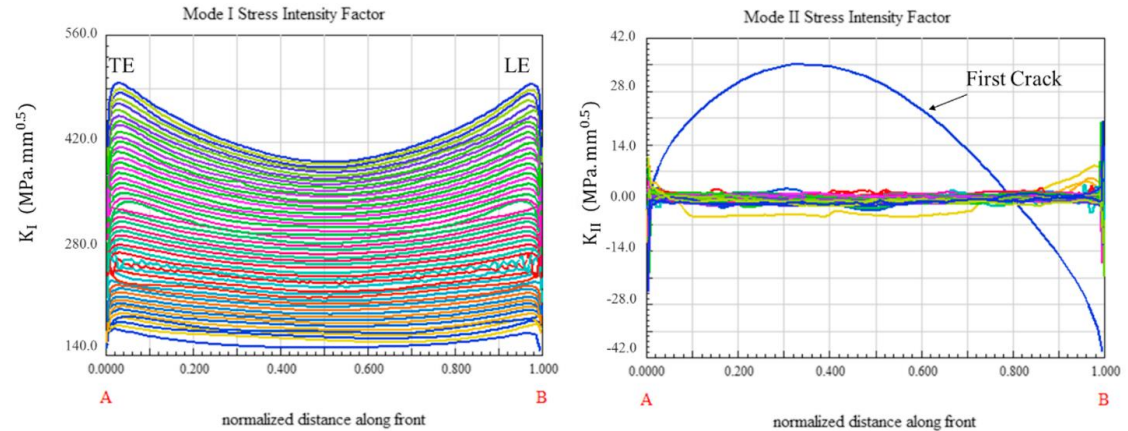
- Transition from short crack to long crack behaviour at $50\ \mu\text{m}$ for Ti alloys [3]
- $125\ \mu\text{m}$ assumed initial crack depth



Minor cycle of 'Descent-Thrust Reverse-Taxi' and a major cycle of 'Start-Takeoff-Shutdown' [1]

Crack growth simulation

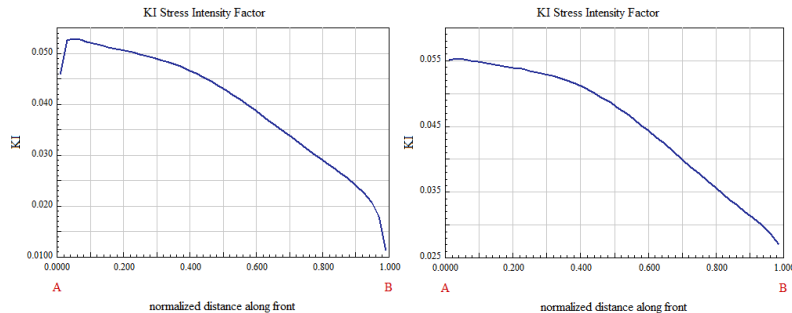
- Crack growth simulation of LCF component completed in FRANC3D + Abaqus
- Crack paths kink to satisfy MTS leading to $\Delta K_{II} = 0$



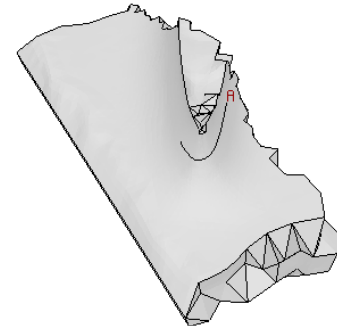
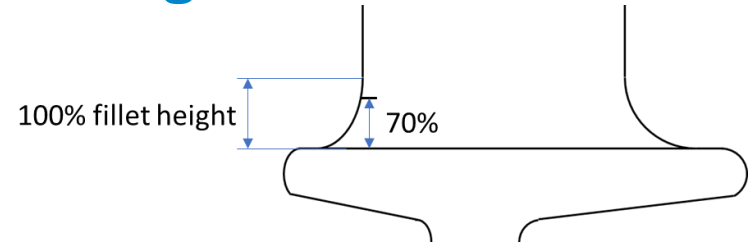
Mode I and II stress intensities along first 55 crack fronts under pure LCF loading (A=TE, B=LE) [1]

Blisk crack propagation – 70% fillet height

- Assumed that loading may be simplified to:
 - Steady: rotational body forces
 - Cyclic: first flap mode vibration
- Inserted semi-elliptical flaw at 70% “fillet height”



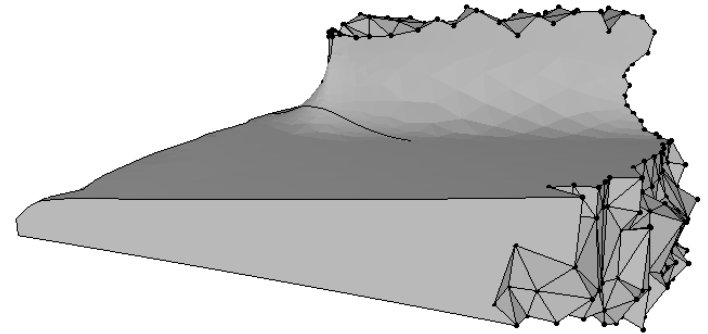
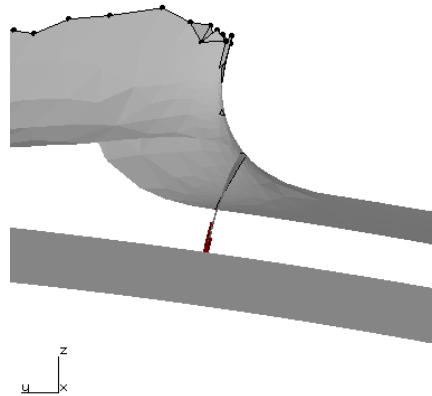
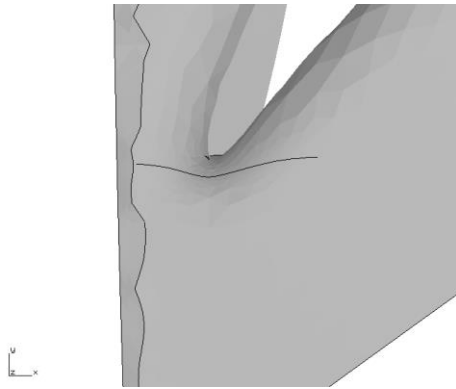
K_I under LC loads for crack growth under consecutive steps



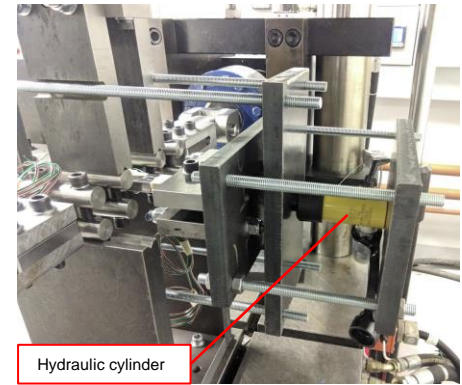
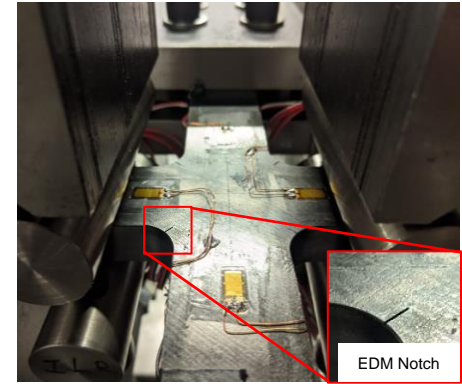
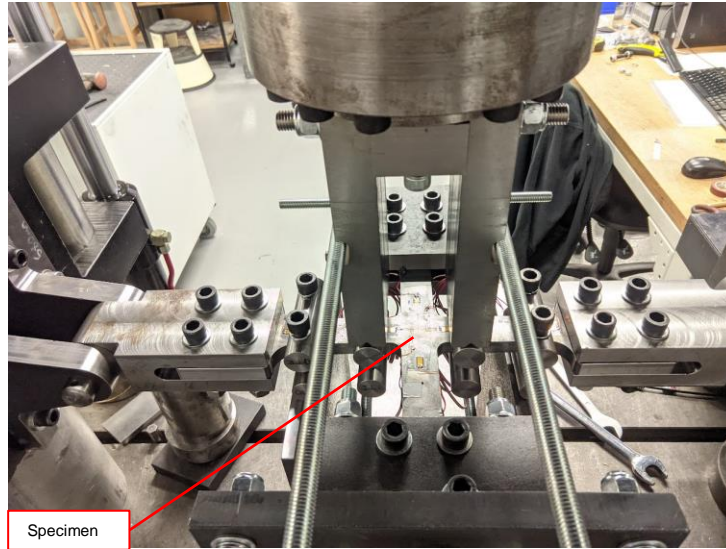
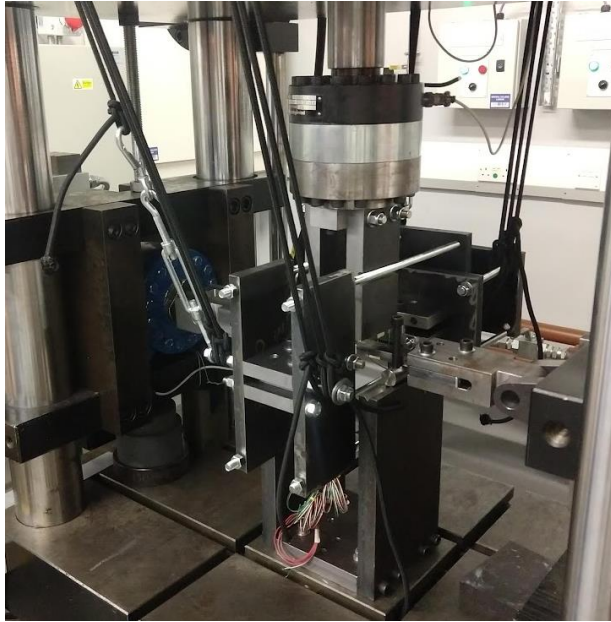
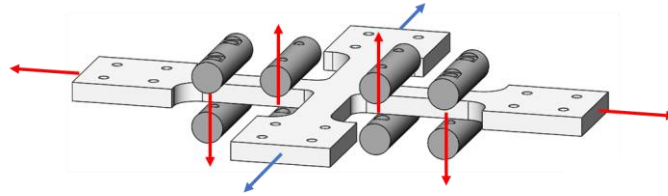
Pressure side labelled 'A'

Blisk crack propagation – 20% fillet height

- Inserted semi-elliptical flaw at 20% “fillet height”
- Immediate growth towards bore

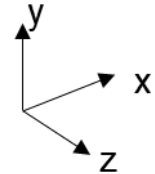
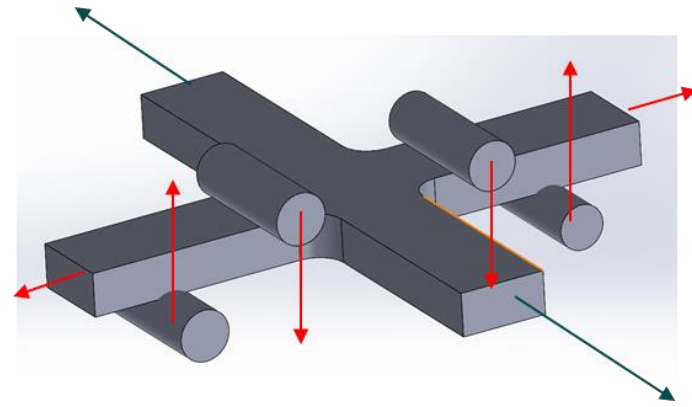
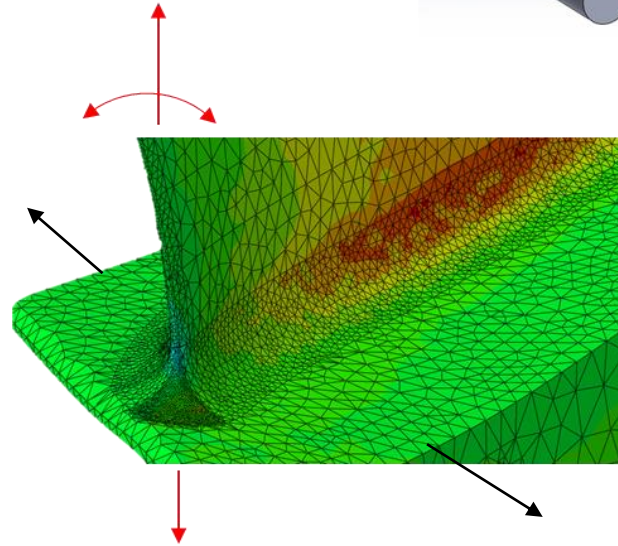


Biaxial test rig



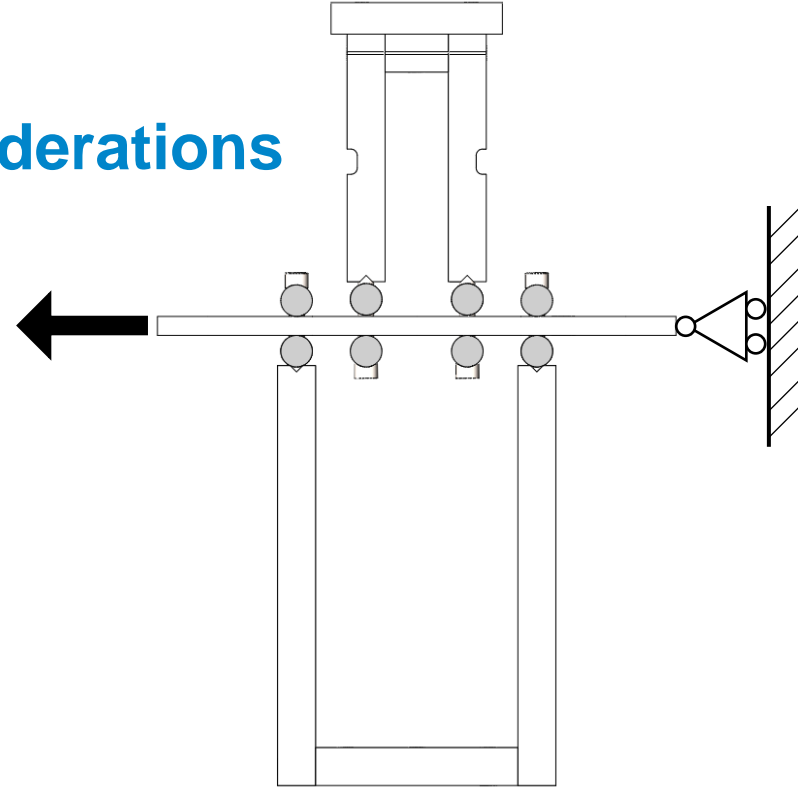
Test sample

- Cruciform sample for biaxial machine
- Tests performed on mild steel S275 and titanium alloy Ti-6Al-4V
- Loading directions
 - X: biaxial machine
 - Y: biaxial machine
 - Z: hydraulic fixture



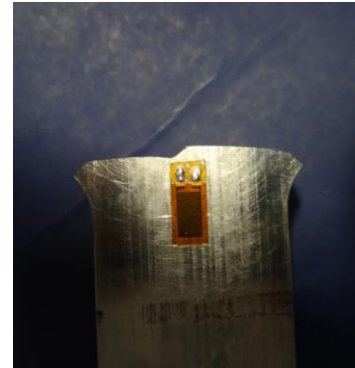
Four-point bending design considerations

- Biaxial machine
 - 1 actuator per axis
 - Specimen is not centred during loading
- Risk of fretting wear at loading pins
 - Requires horizontal compliance

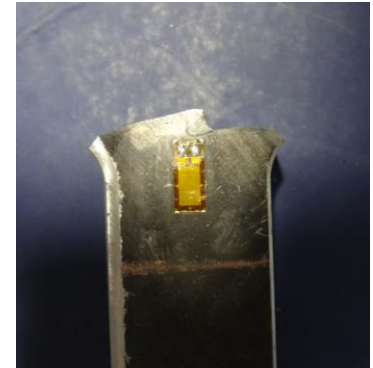


Test settings

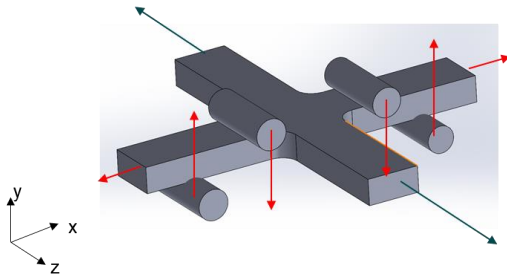
- Loads adjusted to influence crack trajectory



Test 1



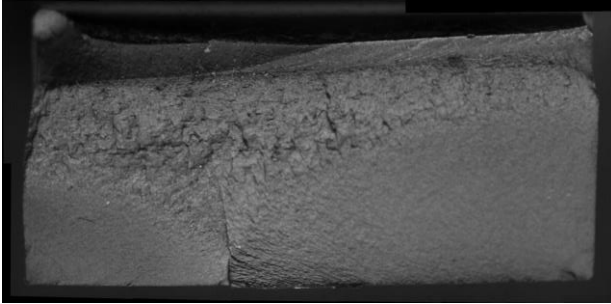
Test 3



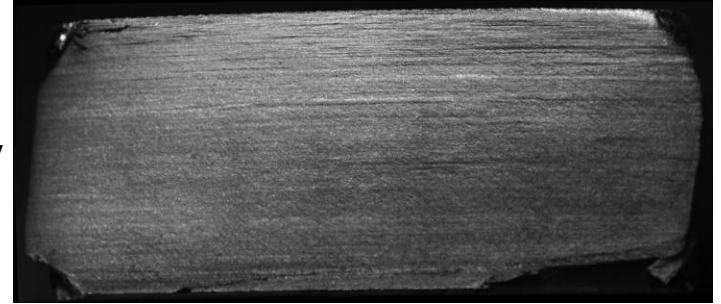
Test Number	Material	x load [kN]	y load (cyclic) [kN]	z load [kN]	N_f
1	Mild steel S275	30.1	14.5	8.7	500,884
2	Ti-6Al-4V	20.1	14.5	8.7	261,306
3	Mild steel S275	20.1	9.5	15.4	839,458
4	Ti-6Al-4V	20.1	9.5	15.4	72,400

Results – fracture surfaces

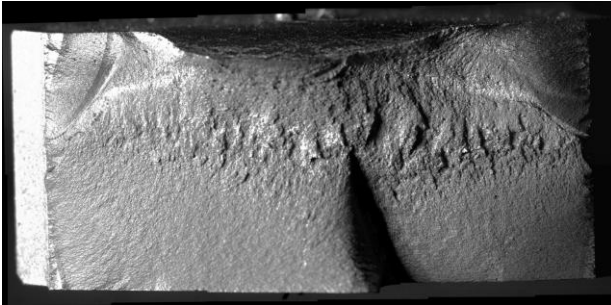
Test 1
Steel S275



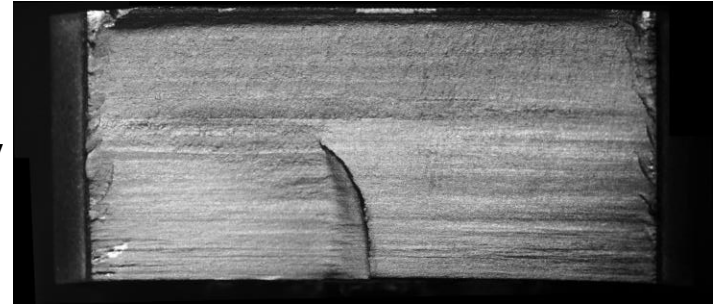
Test 2
Ti-6Al-4V



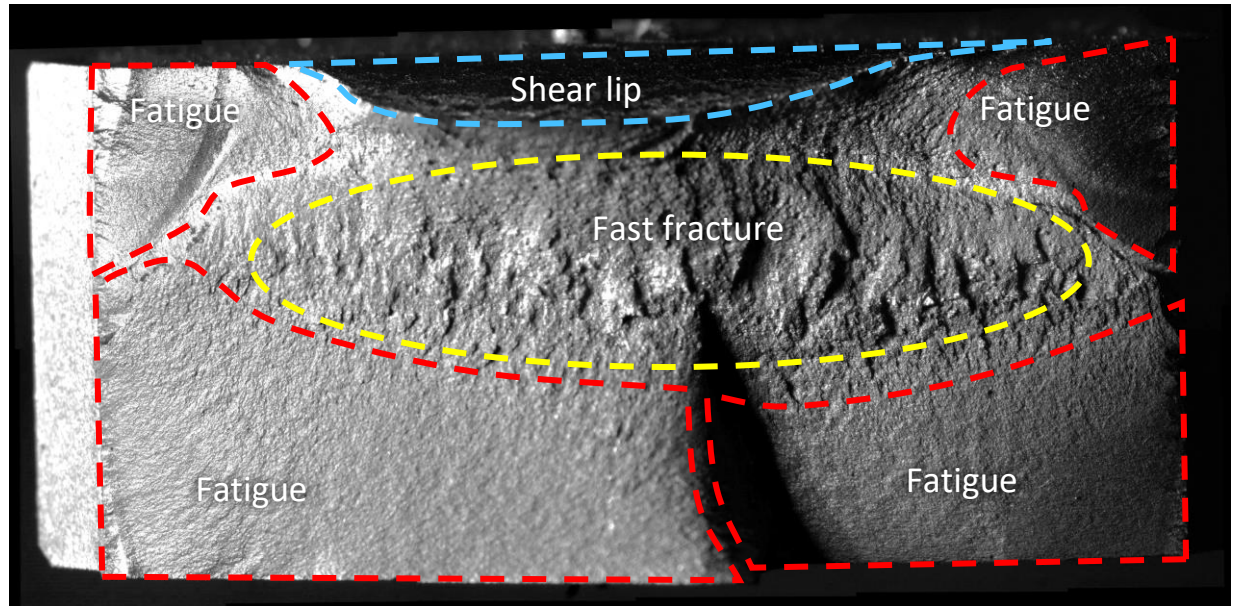
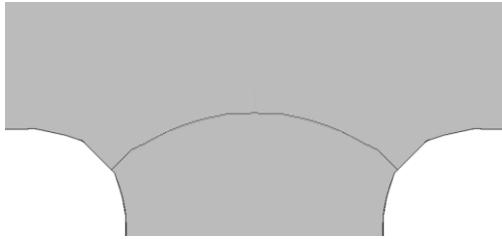
Test 3
Steel S275



Test 4
Ti-6Al-4V

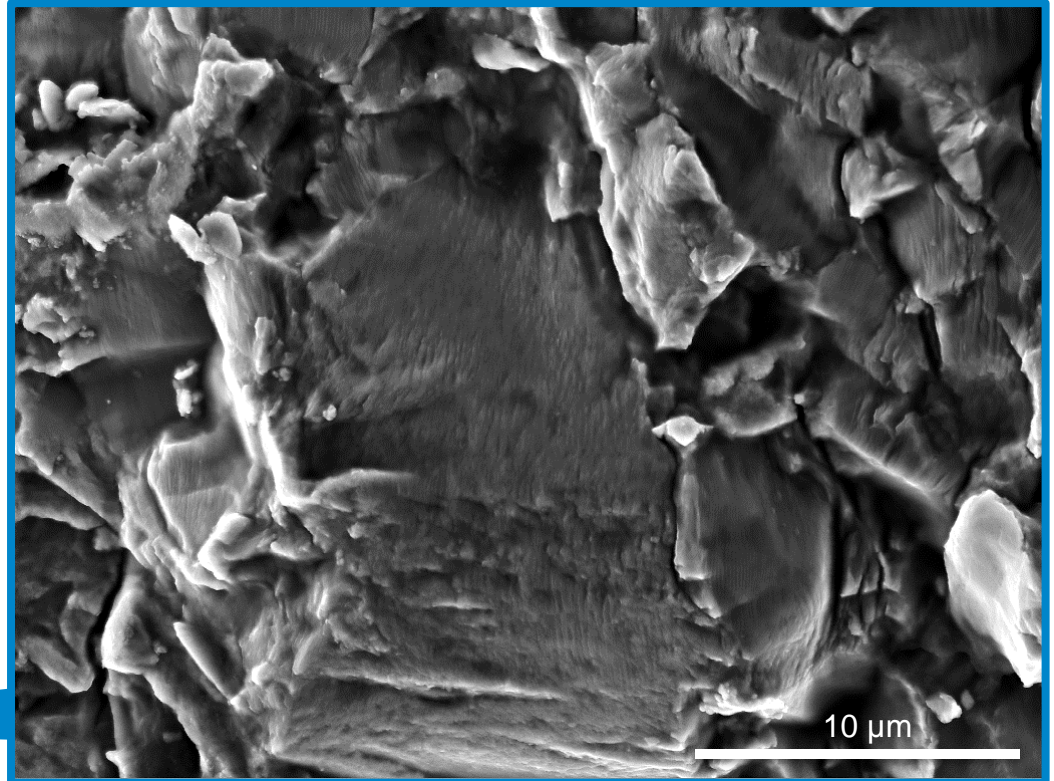
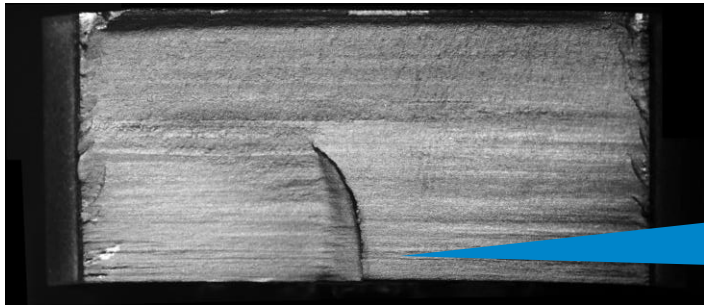


Results – fracture surfaces



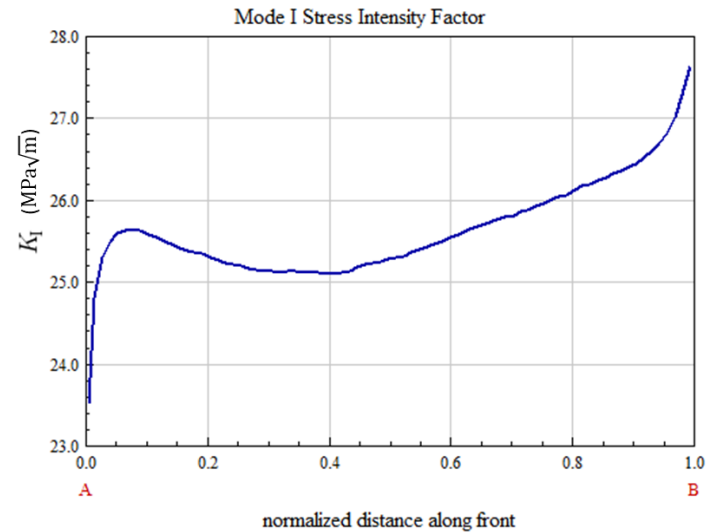
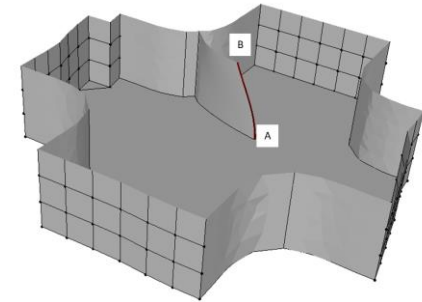
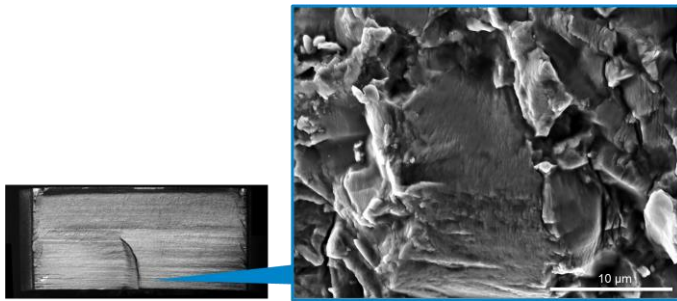
Test 4 fracture surface

- Highly faceted surface due to rolling process
- Striations visible in SEM micrograph



Test 4 fracture surface

- 0.18 μm approximate average striation size in region of interest
- 0.081 μm predicted crack growth per cycle



Summary

- Multiaxial fatigue tests have been completed on notched cruciform specimens
- Directionality of rolled Ti-6Al-4V must be understood further

Future work

- Complete cruciform tests crack deflection angles
- Complete tests with single-notched and double notch specimens
- Complete SENB tests on Ti-6Al-4V specimens to determine directionality of rolled material